Molecular Crystals and Liquid Crystals Science and Technology. Section A. Molecular Crystals and Liquid Crystals

Publication details, including instructions for authors and subscription information:
http://www.tandfonline.com/loi/gmcl19

FIELD DRIVEN HELIX UNWINDING IN THICK AFLC CELLS

Lesley A. Judge [a], Emmanouil E. Kriezis [a] & Steve J. Elston [a]

[a] Department of Engineering Science, Oxford University, Parks Road, Oxford, OX1 3PJ, United Kingdom

Version of record first published: 24 Sep 2006

To cite this article: Lesley A. Judge, Emmanouil E. Kriezis & Steve J. Elston (2001): FIELD DRIVEN HELIX UNWINDING IN THICK AFLC CELLS, Molecular Crystals and Liquid Crystals Science and Technology. Section A. Molecular Crystals and Liquid Crystals, 366:1, 661-671

To link to this article: http://dx.doi.org/10.1080/10587250108024007

Mol. Cryst. and Liq. Cryst., 2001, Vol. 366, pp. 661-671
Reprints available directly from the publisher
Photocopying permitted by license only

Field Driven Helix Unwinding in Thick AFLC Cells

LESLEY A. JUDGE, EMMANOUIL E. KRIEZIS
and STEVE J. ELSTON

Department of Engineering Science, Oxford University, Parks Road, Oxford, OX1 3PJ, United Kingdom

The interaction of the antiferroelectric helix with an electric field applied perpendicular to its axis is investigated. A two stage switching process is observed, in which the helix unwinds to an intermediate state in the pretransitional regime, at voltages below the threshold for antiferroelectric to ferroelectric switching. A series of experimental studies and theoretical modelling show that the intermediate state is an antiferroelectric state in which the directors lie in the plane containing the applied electric field and the smectic layer normal. The mechanism for the unwinding process is the interaction of the applied field with an induced polarisation, which arises from a distortion to the antiferroelectric ordering.

Keywords: antiferroelectric; helix; unwinding; switching; distortion

INTRODUCTION

Antiferroelectric liquid crystals belong to the class of smectic liquid crystals, which have positional order such that the molecules are arranged approximately into layers, forming two-dimensional liquids. In tilted smectics, the orientational order within each layer is such that the average direction of the molecules (the director) is at an angle θ to the layer normal. The c-director is the projection of this director onto the layer, and is described by an azimuthal angle ϕ. Antiferroelectric liquid crystals (AFLCs) have an anticlinic coupling between layers, which causes the c-directors of adjacent layers to be almost anti-parallel [1]. The discrepancy is due to the chirality of the molecules, which causes a small precession of the c-directors from layer to layer, and hence a macroscopic helical structure. In each smectic layer a

spontaneous polarisation exists which is perpendicular to both the normal and the c-director of each layer, and averages to zero in the bulk antiferroelectric phase. When an electric field is applied parallel to the smectic layers, it couples to these polarisations and at sufficiently high fields they all align with each other and the applied field: this is known as the ferroelectric state [2-5]. In this work, however, we primarily concentrate on the 'pre-transitional' switching regime, that is, where the applied field is too low to cause switching to the ferroelectric state.

In understanding the pre-transitional switching behaviour of antiferroelectric liquid crystals (AFLCs), the interaction between the macroscopic helix and the applied electric field is of fundamental importance. However, in many studies of AFLCs, the rôle of the antiferroelectric helix is not clear. This may partly be due to the difficulty in detecting the existence, or otherwise, of a helical structure that generally has a sub-micron pitch. The AFLC mixture CS4001, however, has an unusually long pitch at room temperature (~2.8μm), and the presence of a helical structure is made evident in thick, homogeneously aligned cells, by characteristic dechiralisation lines. This long pitch AFLC is therefore used in this work to study, both experimentally and theoretically, the interaction of the antiferroelectric helix with an electric field applied normal to its axis.

MICROSCOPIC OBSERVATIONS AND LASER SCATTERING

In the ground state of a homogeneously aligned, 11μm cell of AFLC mixture CS4001, the helical superstructure is characterised by dechiralisation lines (see Figure 1(a)) that are spaced by 1.4μm at room temperature, indicating a pitch of 2.8μm. As the field applied to the device is quasi-statically increased within the pre-transitional regime, the dechiralisation lines disappear (see Figure 1(b)) at the same time as the background colour of the texture changes from a dull grey-green colour in the ground state to a bright pink colour. Closer examination of the texture reveals that the switching process is by the growth of fine domains along the direction of the dechiralisation lines. The device remains in this intermediate non-helical, pink state until the threshold field for switching to the ferroelectric state is reached (at about 75V), where domain switching is seen to occur again. In this case, however, the domains are much coarser, bright green striped domains growing into the non-helical pink state. It therefore appears that the helix that is evident in the bulk of the thick cell is unwinding to a non-helical, intermediate state at fields lower than the threshold for switching to the ferroelectric state.

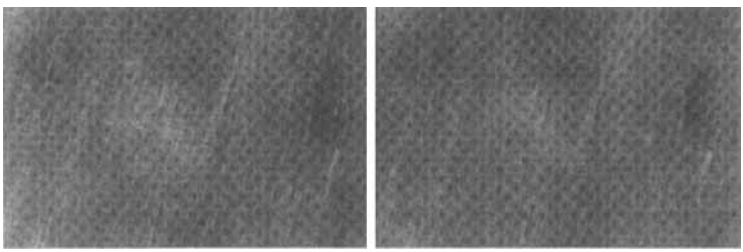

(a) (b)

FIGURE 1 Microscopic observation gives evidence of helix unwinding in the pre-transitional regime: (a) in the ground state, dechiralisation lines separated by 1.4μm indicate the presence of a helical superstructure; (b) in the intermediate state (within the pre-transitional regime), the dechiralisation lines have disappeared.

In order to verify this interpretation of the changes in microscopic texture, the cell was illuminated with a 633nm HeNe laser in the Bragg geometry. Figure 2(a) shows the diffraction that occurs in the ground state due to the periodic variation in refractive indices caused by the helical structure. The diffracted light disappears at voltages that are still below the threshold for switching to the ferroelectric state, as shown in Figure 2(b), confirming that the helical structure is not present in the intermediate state.

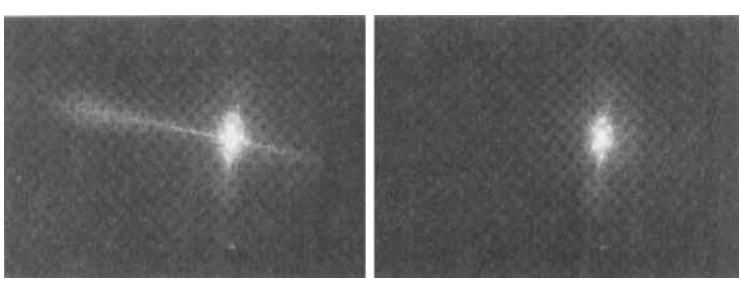

(a) (b)

FIGURE 2 Laser scattering from the cell in the Bragg geometry: (a) in the ground state there is diffraction from the antiferroelectric helix; (b) in the intermediate state, there is no diffraction, confirming that there is no helical structure.

BIREFRINGENCE AND OPTIC AXIS MEASUREMENTS

In order to determine the identity of the intermediate state, the birefringence and optic axis orientation of the cell were measured as a function of applied voltage. At each voltage this was done by illuminating the cell (between crossed polarisers) with a 633nm HeNe laser, and measuring the transmittance as a function of the azimuthal orientation of the cell with respect to the polariser axes. The resulting data follows a sinusoidal variation with the azimuthal angle ψ (see Figure 3(a)), in accordance with:

$$T = \sin^2(2(\psi - \psi_0))\sin^2(\frac{\pi d\Delta n}{\lambda}),$$

where ψ_0 is the angle between the optic axis of the liquid crystal and either of the polarisers, when $\psi = 0$; d is the thickness of the liquid crystal layer in the cell; Δn is the birefringence of the cell at normal incidence, and λ is the wavelength of light used.

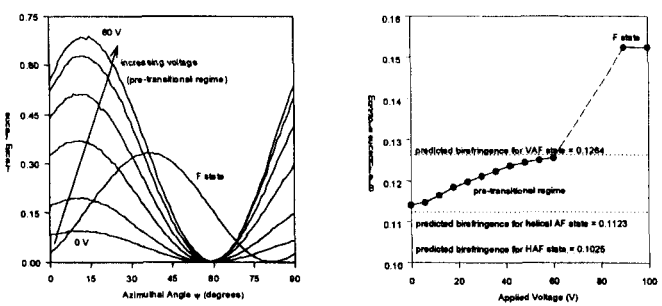

(a) (b)

FIGURE 3 The birefringence and optic axis orientation of the cell were measured as a function of voltage, in order to identify the intermediate state. In the pre-transitional regime, the optic axis hardly rotates at all, whereas the birefringence increases by about 10%. This suggests that the intermediate state is a non-helical antiferroelectric state, with the molecules in the plane parallel to the applied field and the smectic layer normal.

By fitting this formula to the data, Δn and ψ_0 could be determined as a function of voltage. The optic axis orientation of the liquid crystal remains essentially unchanged in the pre-transitional regime, suggesting that the intermediate state is a non-helical antiferroelectric state. Figure 3(b) shows that the birefringence of the material increases by about 10% in the pre-transitional regime, before undergoing a further increase as the antiferroelectric to ferroelectric transition takes place. It therefore appears that the intermediate, non-helical state is a 'vertical' antiferroelectric (VAF) state in which the directors are in the plane defined by the applied field and the smectic layer normal, since this state has a higher birefringence than the helical AF state. The 'horizontal' antiferroelectric (HAF) state in which the directors are in the plane perpendicular to the applied field has a lower birefringence than the helical AF state, and is therefore clear that it cannot be the intermediate state.

This conclusion can also be verified quantitatively, as the birefringence measured for the F state (0.1524) can be used to calculate the expected birefringences of the helical AF, VAF and HAF states to be 0.1122, 0.1265 and 0.1025 respectively. These values are indicated in Figure 3(b), and it is clear that there is good agreement between the ground (0V) and intermediate (60V) states, and the birefringences calculated for the helical AF and VAF states respectively.

The above experiment to measure the birefringence and optic axis orientation assumes that it is possible to assign a single value of birefringence to the helical antiferroelectric state. This may appear to be an over-simplification, given that the pitch of the material is 2.8μm (longer than the wavelength of light) and hence some diffraction might be expected. However, there is very little diffracted light observed at normal incidence (see the laser scattering experiment above, where it was necessary to tilt the cell in order to detect any diffracted light). These observations are consistent with the fact that the Raman-Nath condition ($4d\lambda/np^2<1$) for diffraction at normal incidence is not satisfied for a pitch of 2.8μm and a cell thickness of 11μm. The cell must therefore be in the Bragg geometry in order to observe light diffracted from the helical structure. The lack of diffracted light at normal incidence suggests that it is correct to assign a single value of Δn to the helical structure.

In order to check this hypothesis, the experimental results were compared with the predictions of the Beam Propagation Method (BPM) [6,7]. This is a numerical technique that (by solving Maxwell's equations in the spatial

domain) can predict the propagation of light through a liquid crystal cell that has director variation anywhere in the plane of incidence. It can therefore take into account the helical structure of an AFLC, unlike matrix methods such as those of Jones [8] and Berreman [9]. Using a helical director structure, the program produces the same sinusoidal variation of the transmitted intensity as a function of the azimuthal orientation of the cell, as is obtained experimentally. The 'effective' birefringence that is implied by the numerical output is 0.1123, which differs by less than 0.1% from the birefringence that is measured experimentally of 0.1124. The difference is well within the limits of experimental accuracy, and hence it is concluded that the approximation made in assigning a single value of Δn at normal incidence to the helical structure is a good one.

LASER CONOSCOPY

In order to verify the identity of the intermediate state, the transmittance of the cell between crossed polarisers was measured, this time with a fixed azimuthal angle of 45° between the smectic layer normal and the polariser axes. The cell was rotated in turn both the x (smectic layer normal) and y (parallel to smectic layers and cell surfaces) axes respectively. The experimental results are displayed in Figure 4, together with theoretical predictions for the helical AF, VAF and HAF states, which are used to interpret the results.

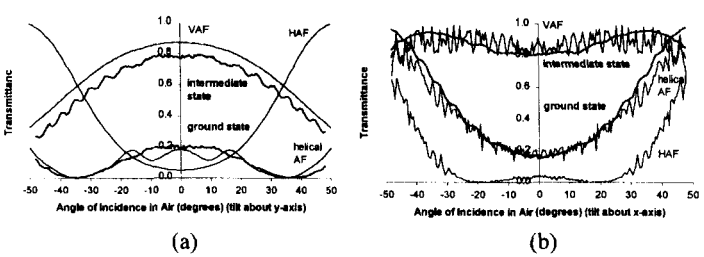

FIGURE 4 Laser conoscopy confirms that the intermediate state is the VAF state. The experimental results (thick lines) for the ground and intermediate states agree with the theoretical predictions (thin lines) for the helical AF and VAF states, respectively.

For tilts about the y axis, the variation in refractive index along the helical (x) axis is in the plane of incidence, and therefore diffraction is expected to

occur as the cell is tilted into the Bragg geometry, as explained above. In this case, therefore, the theoretical predictions are made using the Beam Propagation Method. For the tilts about the x axis, however, the variation of the refractive indices is perpendicular to the plane of incidence, so there is no possibility of tilting the cell into the Bragg geometry. The theoretical predictions given in Figure 4(a), therefore, are the results of a Berreman 4x4 matrix method. For tilts about both x and y axes, the theoretical predictions for the helical AF and VAF states agree with the experimental data for the ground and intermediate states, respectively. The predicted output for the HAF state bears no resemblance to the experimental data. We can therefore confirm with laser conoscopy experiments that the intermediate state is the VAF state.

DIELECTRIC MEASUREMENTS

As the antiferroelectric helix unwinds from the ground state to form the VAF state, we expect to see a change in the low frequency dielectric constant of the material [10,11]. An anti-phase motion of the directors in adjacent layers (that is, a distortion to the antiferroelectric ordering) gives rise to a net polarisation that can couple to an applied electric field, and hence contribute to the dielectric constant of the material. This effect will be at a maximum in the VAF state, since every pair of layers will contribute maximally to the dielectric constant. In the HAF state, there can be no contribution to the dielectric constant from this mode, since the induced polarisation would be perpendicular to the applied field. Similarly, in the ferroelectric state, there can be no further polarisation induced in the direction of the applied field by any additional oscillatory field, hence their can be no contribution from such a mode. In the ground antiferroelectric state, however, the presence of the helical structure suggests that we should expect exactly 50% of the maximum possible contribution to the dielectric constant from this mode, i.e. a total dielectric constant midway between that of the VAF state and the ferroelectric state. We therefore expect that if the antiferroelectric helix does unwind to form the VAF state, then the low frequency dielectric constant should increase in the pre-transitional regime, and then decrease by double that amount during switching to the ferroelectric state. If, however, the helix unwinds to form the HAF state, then the dielectric constant should decrease as the helix unwinds, and remain unchanged during switching to the ferroelectric state. The low frequency (1kHz) dielectric constant of the cell was thus measured as a function of bias voltage, to determine which of the two cases applies, and the results are plotted in Figure 5.

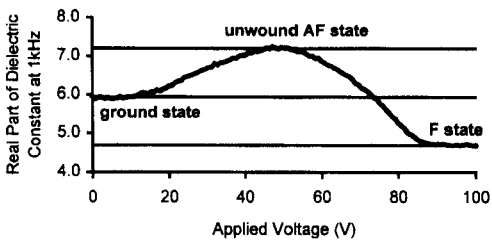

FIGURE 5 The low frequency (1kHz) dielectric constant increases in the pre-transitional regime, and then decreases by double this amount during switching to the ferroelectric state, confirming that the intermediate state is the VAF state.

Figure 5 shows that the dielectric constant first increases as the helix unwinds to the intermediate antiferroelectric state, and then decreases below the initial value as it switches into the ferroelectric state. This confirms once more that the non-helical state is the VAF state. Further, the data is quantitatively correct in that the dielectric constant for the helical antiferroelectric ground state is exactly midway between that of the VAF and ferroelectric states, giving further support to the conclusion that the intermediate state is the VAF state.

THEORETICAL MODEL

In order to both verify the conclusions of the experimental work outlined above, and determine the mechanism for the helix unwinding process observed, the liquid crystal was modelled using the following torque equation:

$$\eta \frac{\partial \phi_i}{\partial t} = -EP_S \sin\phi_i + \frac{\gamma}{2}\sin(\phi_i - \phi_{i+1} + \delta) + \frac{\gamma}{2}\sin(\phi_i - \phi_{i-1} - \delta),$$

where the torque on the director in the i^{th} smectic layer (RHS above) is equated to the product of the viscosity coefficient for motion around the smectic cone (η) and the rate of change of the azimuthal angle around the cone, $d\phi_i/dt$ (LHS above). The first term contributing to the torque (RHS) is the interaction of the electric field (E) with the spontaneous polarisation (P_S) of the i^{th} layer. The second two terms represent the coupling (of strength γ) of

the i^{th} layer with its neighbours, $(i\text{-}1)$ and $(i\text{+}1)$, due to the antiferroelectric ordering that is inherent to this phase of liquid crystal. Note that these contributions to the torque are zero in the ground state when adjacent layers are separated in azimuthal angle by an amount $\pi+\delta$. δ is a small angle, much less than π, that is due to the slow precession of the azimuthal angle of the c-directors from layer to layer that gives rise to the macroscopic helical structure of the phase.

The zero torque solutions are determined numerically as a function of bias field, E, and it is found that as the field increases from zero, the helical structure distorts such that the molecules tend to lie in the plane containing the applied field and the smectic layer normal. This is illustrated for the case $EP_S=\gamma/2$, in Figure 6(a). At this field, there is quite significant distortion of the helix, but very little change to the antiferroelectric ordering, that is, the change in the azimuthal angle difference between adjacent layers does not change significantly. The direction of the helix distortion certainly implies that helix unwinding to the VAF state is possible. In order to verify this, the energy of the cell was plotted as a function of applied field, and compared with that in which the starting state is the VAF state, rather than the helical antiferroelectric state (shown in Figure 6(b)). At zero applied field, the helical state is lower in energy than the VAF state, but at higher fields there is a cross-over. The presence of defects in the cell ensures that the lowest energy state will eventually be occupied even in the presence of an energy barrier between initial and final states (via a process of defect seeded domain switching, as observed under the microscope). Hence theory predicts helix distortion, and eventually helix unwinding in the pre-transitional regime.

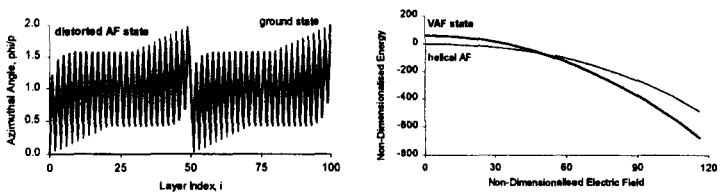

(a) (b)

FIGURE 6 The theoretical model predicts helix distortion as shown in (a), and eventually helix unwinding to the VAF state, as shown by the cross-over in energies in (b).

The mechanism for the helix unwinding process can be usefully understood as follows. In Figure 6(a), although the dominant change to the helical antiferroelectric state is a rotation of the directors in each layer such that the molecules tend to lie in a plane parallel to the electric field, there is some distortion to the antiferroelectric ordering, and it is this that allows the helix unwinding to occur. Once a distortion to the antiferroelectric ordering has occurred, there exists a net polarisation, which then couples to the applied field, and allows the helix distortion that we observe. Since this induced polarisation between a pair of layers is in a direction parallel to their average c-director, and this tends to rotate to align with the electric field, then the non-helical state that eventually occurs has the c-directors parallel to the applied field. We thus understand both the mechanism for helix distortions, and the reason that the non-helical, intermediate antiferroelectric state is the VAF state rather than the HAF state. It is interesting to note that the wavelength of the helix distortion is one half of the helical pitch, which is consistent with the symmetry of the AFLC phase.

CONCLUSIONS

A series of experimental and theoretical investigations have been carried out in order to understand the interaction between the antiferroelectric helix and an electric field applied perpendicular to its axis. Microscopic observations and laser scattering studies show that the antiferroelectric helix unwinds to an intermediate state as the applied field increases within the pre-transitional regime. Birefringence and optic axis orientation measurements suggest that the intermediate state is an antiferroelectric state in which the molecules lie in a plane that is parallel to the applied field and the smectic layer normal (the 'vertical' AF state of 'VAF' state). This identification was verified by laser conoscopy and dielectric experiments. A theoretical model supported these conclusions by showing that as the applied field increases, the directors rotate (whilst maintaining approximate antiferroelectric ordering) to align with the applied field. The mechanism for this rotation is the interaction between the applied field and an 'induced' polarisation that arises from a distortion to the antiferroelectric ordering. Since the induced polarisation is in a direction parallel to the c-directors, the final non-helical state has the c-directors parallel to the applied field, i.e. the molecules lie in the plane defined by the electric field and the smectic layer normal (the VAF state). The induced polarisation repeats every half pitch through the helical structure, in agreement with the symmetry of the AFLC phase.

ACKNOWLEDGEMENTS

The authors would like to acknowledge the financial support of the EPSRC and the provision of a CASE award and test cells by Sharp Laboratories of Europe, Oxford.

References

[1] A. Chandani et al.: *Jpn. J. Appl. Phys.*, **27**, L729 (1988) **28**, L1261 (1989) **28**, L1265 (1989).
[2] M. Johno, A. Chandani, J. Lee, Y. Ouchi, H. Takezoe, A. Fukuda, K. Itoh, T. Kitazume: *Proceedings of the SID*, **31**, 2, 129 (1990).
[3] M. Johno, K. Itoh, J. Lee, Y. Ouchi, H. Takezoe, A. Fukuda, T. Kitazume: *Jpn. J. Appl. Phys.*, **29**, 1, L107 (1990).
[4] J. Lee, A. Chandani, K. Itoh, Y. Ouchi, H. Takezoe, A. Fukuda: *Jpn. J. Appl. Phys.*, **29**, 6, 1122 (1990).
[5] A. Fukuda, Y. Takanishi, T. Isozaki, K. Ishikawa, H. Takezoe: *J. Mater. Chem.*, **4**, 7, 997 (1994).
[6] E. Kriezis, S. Elston: *J. Modern Optics*, **46**, 1201–1212 (1999).
[7] E. Kriezis, S. Elston: accepted by *Applied Optics*.
[8] R. Jones, *J. Opt. Soc. Am.* **62**, 488–493 (1941).
[9] D. Berreman, *J. Opt. Soc. Am.* **62**, 502–510 (1972).
[10] Y. Panarin, O. Kalinovskaya, J. Vij: *Liquid Crystals*, **25**, 2, 241 (1998).
[11] M. Buivydas et al.: *Liquid Crystals*, **18**, 6, 879 (1995) **23**, 5, 723 (1997).